Title

Evaluation of enamel surface modification using PS-OCT after laser treatment to increase resistance to demineralization

Authors

Kim, Jin Wan
Chan, Kenneth H
Fried, Daniel

Publication Date

2016-02-29

DOI

10.1117/12.2218662

Peer reviewed

HHS Public Access

Author manuscript

Proc SPIE Int Soc Opt Eng. Author manuscript; available in PMC 2016 March 20.

Published in final edited form as:

Proc SPIE Int Soc Opt Eng. 2016 February 13; 9692: . doi:10.1117/12.2218662.

Evaluation of enamel surface modification using PS-OCT after laser treatment to increase resistance to demineralization

Jin Wan Kim, **Kenneth H. Chan**, and **Daniel Fried**[1]

University of California, San Francisco, San Francisco, CA 94143-0758

Abstract

At laser intensities below ablation, carbonated hydroxyapatite in enamel is converted into a purer phase hydroxyapatite with increased acid resistance. Previous studies suggested the possibility of achieving the conversion without surface modification. This study attempts to evaluate the thresholds for the modification without additional changes in physical and optical properties of the enamel. Bovine specimens were irradiated using an RF-excited CO_2 laser operating at 9.4-μm with a pulse duration of 26-μs, pulse repetition rates of 100–1000 Hz, with a Gaussian spatial beam profile - 1.4 mm in diameter. After laser treatment, the samples were subjected to acid demineralization for 48 hours to simulate acidic intraoral conditions of a caries attack. The resulting demineralization and erosion were assessed using polarization sensitive OCT (PS-OCT) and 3D digital microscopy. The images from digital microscopy demonstrated a clear delineation between laser protected zones without visual changes and zones with higher levels of demineralization and erosion. Distinct changes in the surface morphology were found within the laser treated area in accordance with the Gaussian spatial beam profile. There was significant protection from the laser in areas that were not visually altered.

Keywords

optical coherence tomography; caries prevention; carbon dioxide laser

1. INTRODUCTION

Previous studies indicated that CO_2 laser irradiation renders enamel more resistant to acid dissolution. At wavelengths between 9–11 μm where CO_2 lasers operate, enamel strongly absorbs laser energy resulting in the conversion of carbonated hydroxyapatite to a purer phase hydroxyapatite [1–5]. In this study, we test the hypothesis that caries inhibition can be imparted without changing the appearance of the enamel surface. Optical coherence tomography is capable of measuring dimensional changes nondestructively on tooth surfaces. It appears to be an ideal tool for monitoring tooth erosion, which is the removal and softening of tooth surfaces due to a variety of factors including subsurface demineralization [6].

[1]daniel.fried@ucsf.edu.

Previous studies have also shown that polarization sensitive optical coherence tomography (PS-OCT) can nondestructively measure the severity of subsurface demineralization in enamel and dentin and is therefore well suited for this role [7–9]. Since OCT measures changes in the reflectivity of the enamel it is capable of measuring both changes in the enamel due to thermal modification by laser irradiation and changes in the reflectivity due to acid demineralization.

In a previous study, we demonstrated that PS-OCT could be used to nondestructively assess caries inhibition after carbon dioxide laser irradiation and the application of topical fluoride [10]. PS-OCT was used to measure the integrated reflectivity of the lesion area and it was significantly lower in the laser and fluoride treated areas. We also found that the laser irradiation alone caused changes in the reflectivity of the enamel and caused an increase in the integrated reflectivity from those areas. This interfered with assessment of the enamel lesions but was not large enough to prevent resolution of differences between the treated and untreated groups. It appeared that at incident fluence below the melting threshold for enamel at the "wings" of the laser treated zones where there were minimal changes in enamel reflectance, the laser was still effective in inhibiting demineralization. The purpose of this study was to follow up on that prior study using a new RF-excited laser operating at 9.4-μm that is capable of generating short 26-μs laser pulses with high single pulse energies (>100-mJ) delivered at high pulse repetition rates. With the Gaussian spatial profile and the high single pulse energies a large beam diameter (~ 1.4 mm) can be used. The thresholds for surface modification (changes in reflectivity) and resistance to acid dissolution were assessed with varying fluence using PS-OCT.

2. MATERIALS AND METHODS

2.1 Sample Preparation

Sixteen bovine enamel blocks, approximately 10 mm in length, 2-mm in width, and a thickness of ~1 mm of bovine enamel were prepared from extracted tooth incisors acquired from a slaughterhouse. Each enamel sample was partitioned into three regions or windows (two laser irradiated, and one protected) by etching 140 μm wide incisions 2-mm apart across each of the enamel blocks (see Fig. 1). Fluence values of 1.6 and 2.6 J/cm^2 were used. In the center a thin layer of acid resistant varnish, red nail polish, Revlon (New York, NY) was applied to protect the sound enamel control area. The center window was left unprotected.

All samples were exposed to a surface softened demineralization solution composed of a 40-ml aliquot of 2.0 mmol/L calcium, 2.0 mmol/L phosphate, and a 0.075 mol/L acetate at pH 4.8 at 37 °C for 48 hours. After exposure the acid resistant varnish was removed with acetone, Fisher Scientific (Hampton, NH) and then scanned with PS-OCT.

2.2 Laser Irradiation Parameters

An RF-excited laser prototype, Diamond J5-V from Coherent (Santa Clara, CA) operating at a wavelength of 9.4 μm was used with a pulse duration of 26-μs and pulse repetition rates of up to 3 kHz. The laser had a Gaussian shaped spatial profile. The laser energy output was

monitored using a power/energy meter, ED-200 from Gentec (Quebec, Canada). The laser beam was focused to a beam diameter of 1.4 mm using a ZnSe scanning lens of f=125-mm. A razor blade was scanned across the beam to determine the diameter ($1/e^2$) of the laser beam. A computer-controlled stage high-speed motion control system with Newport (Irvine, California) UTM150 and 850G stages and an ESP300 controller was used to create controlled movement of the samples during laser irradiation. Samples were scanned across the laser beam at the rate of 2 mm/sec and the pulse repetition rate was varied. Incisions separating the windows were created using the same laser system but a f=25-mm aspheric ZnSe lens was used to create incision ~ 140-μm in diameter. A low volume/low pressure air-actuated fluid spray delivery system consisting of a 780S spray valve, a Valvemate 7040 controller, and a fluid reservoir from EFD, Inc. (East Providence, RI) was used to provide a uniform spray of fine water mist onto the tooth surfaces at 2 mL/min.

2.3 PS-OCT System

An all-fiber-based optical coherence domain reflectometry (OCDR) system with polarization maintaining (PM) optical fiber, high-speed piezoelectric fiber-stretchers and two balanced InGaAs receivers that was designed and fabricated by Optiphase, Inc., Van Nuys, CA was used. This two-channel system was integrated with a broadband superluminescent diode (SLD) Denselight (Jessup, MD) and a high-speed XY-scanning system (ESP 300 controller and 850G-HS stages, National Instruments, Austin, TX) for *in vitro* optical tomography. This system is based on a polarization-sensitive Michelson white light interferometer. The high power (15 mW) polarized SLD source operated at a center wavelength of 1317 nm with a spectral bandwidth full-width at half-maximum (FWHM) of 84 nm. The sample arm was coupled to an AR-coated fiber-collimator to produce a 6-mm in diameter, collimated beam. That beam was focused onto the sample surface using a 20-mm focal length AR-coated planoconvex lens. This configuration provided lateral resolution of approximately 20-μm and an axial resolution of 10-μm in air with a signal to noise ratio of greater than 40–50 dB. The PS-OCT system is completely controlled using Labview software from National Instruments (Austin, TX). The system is described in greater detail [11, 12]. Acquired scans are compiled into *b-scan* files. Image processing was carried out using Igor Pro, data analysis software from Wavemetrics Inc. (Lake Oswego, OR).

2.4 Analysis of PS-OCT Scans

In previous studies [13–15], we established automated methods for determining the depth of demineralization (LD) and integrating over that depth to calculate the integrated reflectivity with depth which we call (ΔR) which is analogous to the integrated mineral loss called ΔZ which is measured with microradiography and is the gold standard for quantification of the severity of demineralization. The demineralization can be represented by 2D projection maps of LD and ΔR. In this study, LD and ΔR maps were created for all the windows, both after laser irradiation and after exposure to the demineralization. Lineouts were extracted at 0, 300, 600, 900, 1200, and 1500-μm from the center of the irradiated spot in LD and ΔR maps for comparing the changes with laser intensity along the laser profile. If erosion was present, erosion depths were calculated by comparing the heights of the demineralized, laser treatment window and acid-resistant control using 3 randomly chosen 2D PS-OCT cross-sectional B-scans. The ΔR was calculated using an estimated ΔR value for the erosion (depth

multiplied with the highest reflectivity) and added to the ΔR values from the 2D projections maps.

3. RESULTS AND DISCUSSION

A depth convolution digital image of the surface of one of the bovine blocks irradiated at 1.6 J/cm^2 with a 100 Hz repetition rate and a scanning speed of 2 mm/sec is shown in Fig. 2 and there are different zones of surface modification that are clearly visible. On the right side of the image (Area 4) at the center of the laser beam the enamel has been completely melted producing wave-like structures and a glazed appearance to the enamel. The surface is modulated with the wavelike structures with a modulation of ±10–20-μm. In area 3, the enamel appears whiter and the overall reflectivity is higher and the enamel appears to be separated into large grains. The appearance is very similar to the dried mud in a lake bed. In Area 2, the craze lines are smaller and close inspection shows that the visibility of the enamel prism boundaries is enhanced as if they were etched and the area appears darker due to the diffuse scattering at the prism boundaries. Thermal analysis studies have shown that enamel melts at 1200°C, and that thermal decomposition of carbonated hydroxyapatite to purer phase hydroxyapatite occurs at 420°C [16]. These changes are expected to increase the acid resistance of enamel [1, 17]. In addition changes to protein and lipid such as denaturation take place at much lower temperatures, above 80°C [18, 19]. It is likely that Area 4 represents temperature excursions exceeding 1200°C, area 2 represents temperatures exceeding 420 °C causing thermal decomposition and the lattice contraction that produces the craze lines and granular appearance. Protein and lipid is concentrated at the prism boundaries so it is likely that enhancement of the prism boundaries in area 2 occurs at temperatures between 80–420 °C and it does appear that the magnitude of the changes varies considerably across area 2, with the right side appearing darker. Depth convolution images are shown in Fig. 3 for a sample irradiated at 2.6 J/cm^2 with a 100 Hz repetition rate and a scanning speed of 2 mm/sec. The melted zone is more extensive for the higher fluence. After exposure to the demineralization solution the unprotected areas were eroded while the laser treated areas remained intact. In between the eroded area and the melted area there is a protected zone that remained intact.

The integrated reflectivity is plotted for each position in Fig. 4 after laser irradiation and after exposure to the demineralization solution for the samples irradiated at 2.6 J/cm^2 with a 100 Hz repetition rate and a scanning speed of 2 mm/sec. In the top plot representing the reflectivity changes created by the laser, the reflectivity is significantly higher than the non-irradiated area out to 300-μm from the center. After exposure to the demineralization the laser irradiated zones out to 900-μm had a significantly lower reflectivity than the non-irradiated zone (1200-μm) indicating that the areas with minimal surface modification (600 & 900-μm) provided additional protection against acid dissolution.

In summary, there was significant protection from the laser in areas that were not visually altered. By utilizing the laser beam intensity profile, we can determine the incident fluence necessary for protection while not markedly altering the surface reflectivity.

Future studies will focus on providing uniform surface treatments without altering reflectivity using the thresholds identified in this study.

Acknowledgments

We would like to thank Robert Lee for his contributions and acknowledge the support of Dr. George Taylor and NIH/NIDCR grants R01- DE017869 and R01-DE019631.

REFERENCES

1. Fowler B, Kuroda S. Changes in heated and in laser-irradiated human tooth enamel and their probable effects on solubility. Calcif Tissue Int. 1986; 38:197–208. [PubMed: 3011230]
2. Featherstone JDB, Nelson DGA. Laser effects on dental hard tissue. Adv Dent Res. 1987; 1(1):21–26. [PubMed: 3125842]
3. Nelson DGA, Jongebloed WL, Featherstone JDB. Laser irradiation of human dental enamel and dentine. NZ Dent J. 1986; 82:74–77.
4. Featherstone JDB, Barrett-Vespone NA, Fried D, Kantorowitz Z, Lofthouse J. CO_2 laser inhibition of artificial caries-like lesion progression in dental enamel. J Dent Res. 1998; 77(6):1397–1403. [PubMed: 9649168]
5. Fried D, Murray MW, Featherstone JDB, Akrivou M, Dickenson KM, Duhn C. Dental hard tissue modification and removal using sealed TEA lasers operating at λ=9.6 μm. J Biomed Optics. 2001; 6(2):231–238.
6. Lussi, A. Dental Erosion:From Diagnosis to Therapy KARGER. New York: 2006.
7. Baumgartner A, Dicht S, Hitzenberger CK, Sattmann H, Robi B, Moritz A, Sperr W, Fercher AF. Polarization-sensitive optical optical coherence tomography of dental structures. Caries Res. 2000; 34:59–69. [PubMed: 10601786]
8. Fried D, Xie J, Shafi S, Featherstone JDB, Breunig T, Lee CQ. Early detection of dental caries and lesion progression with polarization sensitive optical coherence tomography. J Biomed Optics. 2002; 7(4):618–627.
9. Lee C, Darling C, Fried D. Polarization Sensitive Optical Coherence Tomographic Imaging of Artificial Demineralization on Exposed Surfaces of Tooth Roots. Dent Mat. 2009; 25(6):721–728.
10. Hsu DJ, Darling CL, Lachica MM, Fried D. Nondestructive assessment of the inhibition of enamel demineralization by CO_2 laser treatment using polarization sensitive optical coherence tomography. J Biomed Optics. 2008; 13(5):054027.
11. Bush J, Davis P, Marcus MA. All-Fiber Optic Coherence Domain Interferometric Techniques. Fiber Optic Sensor Technology II. Proc SPIE. 2000; 4204:71–80.
12. Ngaotheppitak P, Darling CL, Fried D, Bush J, Bell S. PS-OCT of Occlusal and Interproximal Caries Lesions viewed from Occlusal Surfaces. Lasers in Dentistry XII. 2006; 6137(L):1–9.
13. Chan KH, Chan AC, Fried WA, Simon JC, Darling CL, Fried D. Use of 2D images of depth and integrated reflectivity to represent the severity of demineralization in cross-polarization optical coherence tomography. J Biophotonics. 2015; 8(1–2):36–45. [PubMed: 24307350]
14. Arends J, Ruben JL, Inaba D. Major topics in quantitative microradiography of enamel and dentin: R parameter, mineral distribution visualization, and hyper-remineralization. Adv Dent Res. 1997; 11(4):403–414. [PubMed: 9470497]
15. Le MH, Darling CL, Fried D. Automated analysis of lesion depth and integrated reflectivity in PS-OCT scans of tooth demineralization. Lasers Surgery Med. 2010; 42(1):62–68.
16. Holcomb DW, Young RA. Thermal decomposition of human tooth enamel. Calcif Tissue Int. 1980; 31:189–201. [PubMed: 6258760]
17. Kuroda S, Fowler BO. Compositional, structural and phase changes in *in vitro* laser-irradiated human tooth enamel. Calcif Tissue Int. 1984; 36:361–369. [PubMed: 6435835]
18. Pearce, J.; Thomsen, S. Rate Process Analysis of Thermal Damage. Plenum, NY: 1995.
19. Welch AJ. The Thermal Response of Laser Irradiated Tissue. IEEE J Quantum Electronics. 1984; 20(12):1471.

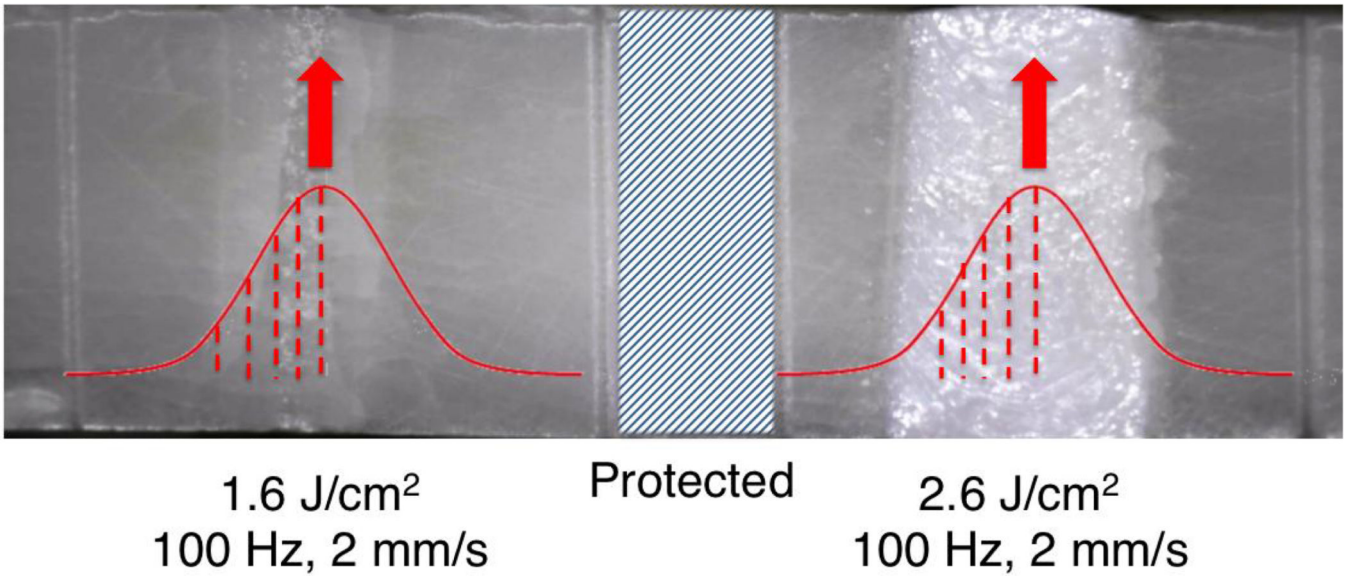

Fig. 1.
Bovine enamel block with the 2 treatment windows with a superimposed diagram of the incident fluence distribution for different irradiation parameters.

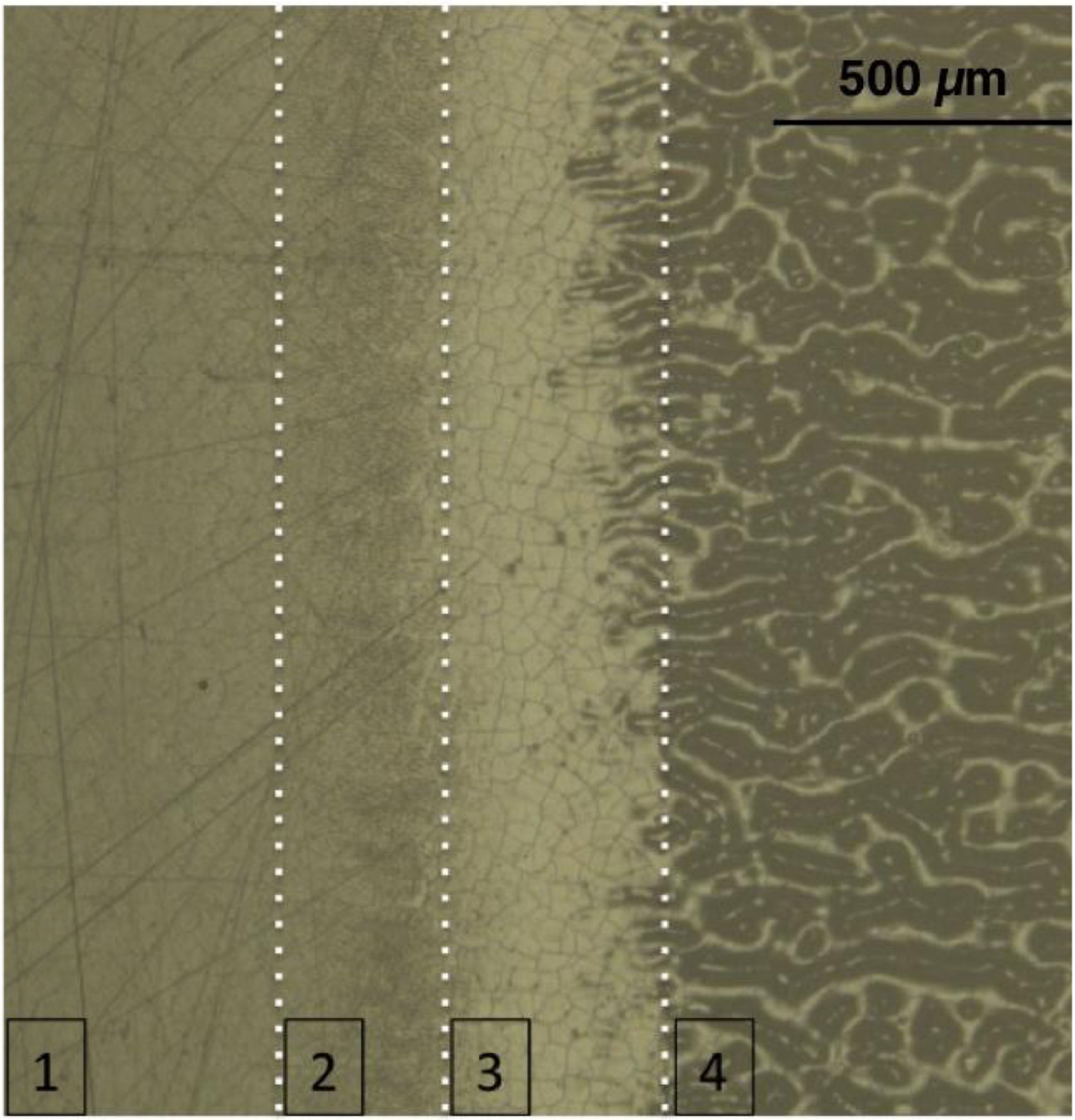

Fig. 2.

Depth convolution image showing different surface modification from center of the laser profile (4) to unaffected area (1). Sample irradiate with fluence of 1.6 J/cm^2 with a 100 Hz repetition rate and a scanning speed of 2 mm/sec.

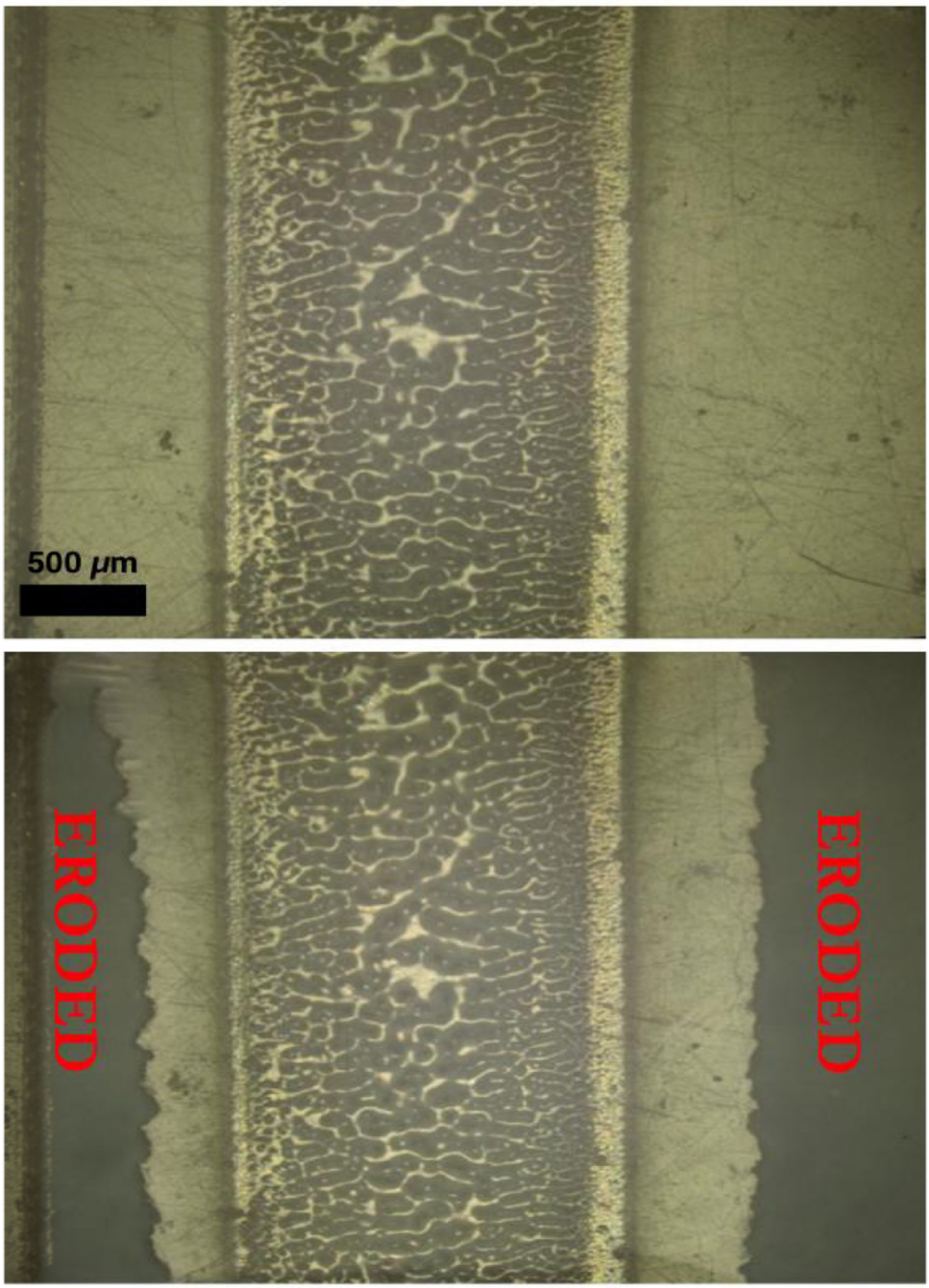

Fig. 3.

Depth convolution images after laser irradiation (top) and after exposure to the demineralization solution (bottom). Sample irradiated with fluence of 2.6 J/cm^2, 100 Hz repetition rate, and a scanning speed of 2 mm/sec.

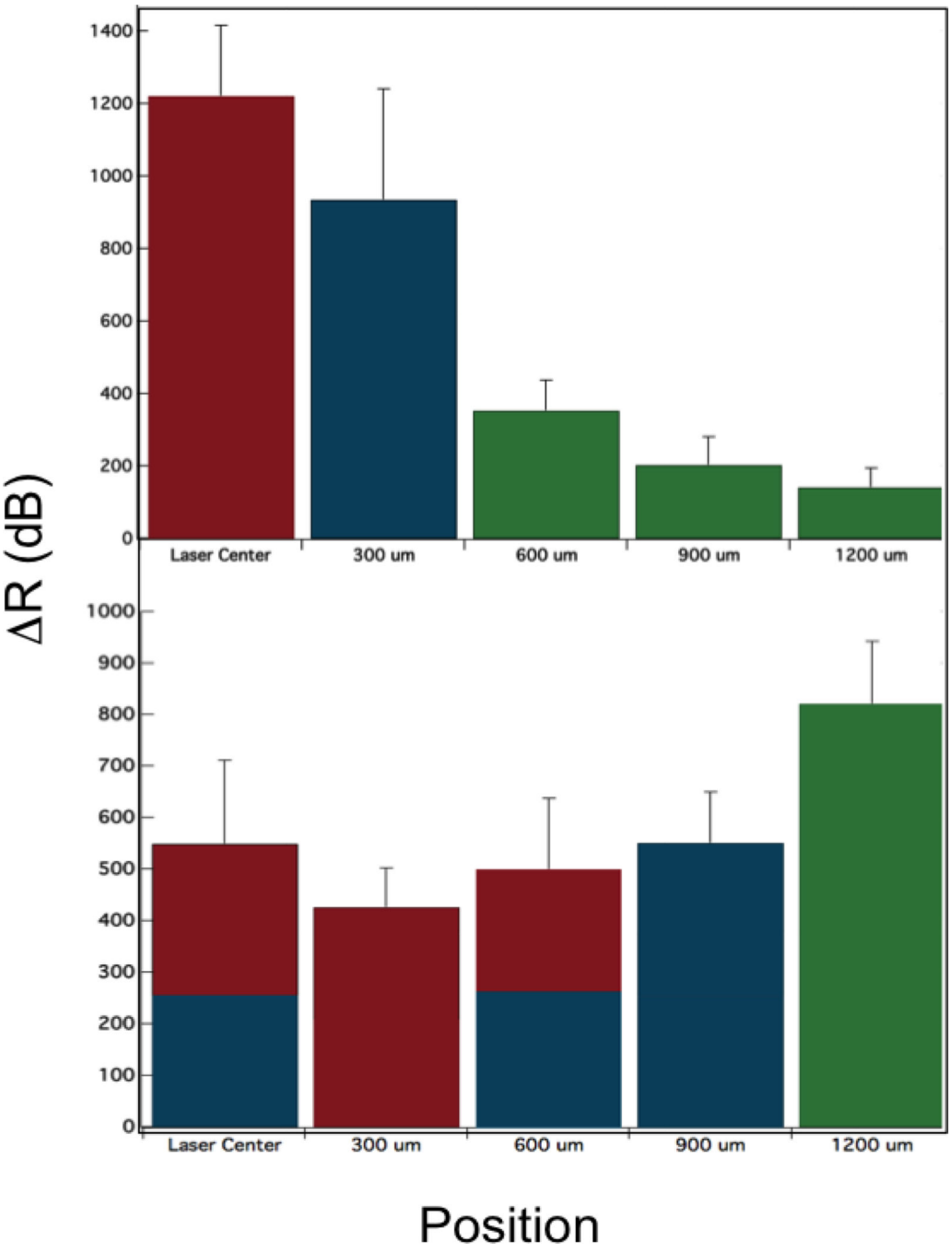

Fig. 4.

Measured mean integrated reflectivity ± S.D. before (top) and after laser irradiation and exposure to the demineralization solution (bottom) with varying distance from the laser center. Bars of the same color are statistically similar (P>0.05). There were eight samples per group.